J|A|C|S
ARTICLES
Published on Web 05/23/2006

Quenching of the Electrochemiluminescence of Tris(2,2′-bipyridine)ruthenium(II) by Ferrocene and Its Potential Application to Quantitative DNA Detection

Weidong Cao,[†] Jerome P. Ferrance,[†] James Demas,[†] and James P. Landers*[,†,‡]

Contribution from the Department of Chemistry, University of Virginia, Charlottesville, Virginia 22904, and Department of Pathology, University of Virginia Health Science Center, Charlottesville, Virginia 22908

Received January 9, 2006; E-mail: landers@virginia.edu

Abstract: Efficient and stable quenching of electrochemiluminescence (ECL) of tris(2,2′-bipyridine)-ruthenium(II) by oxidizing ferrocene methanol (FcMeOH) at the electrode is reported. Bimolecular energy or electron transfer between $Ru(bpy)_3^{2+*}$ and ferrocenium (Fc^+), the oxidized species of Fc, along with suppression of radical reactions is suggested as the mechanism for quenching ECL. Fc shows more efficient quenching of ECL compared with the known quenchers phenol and 1,1-dimethyl-4,4′-bipyridine dication (MV^{2+}). The ECL quenching rate constant was 5.6×10^{10} M^{-1} s^{-1}. Using Fc as a quencher label on a complementary DNA sequence, an intramolecular ECL quenching in hybridized oligonucleotide strands has been realized. With essentially complete quenching efficiency, this system has the potential for application to sequence-specific DNA detection.

Introduction

Electrochemiluminescence (ECL) of tris(2,2′-bipyridyl)ruthenium(II) ($Ru(bpy)_3^{2+}$) is a well-known detection method that provides high sensitivity with low background through generation of an optical signal triggered by an electrochemical reaction. This detection method has been utilized in a number of bioanalytical arenas, including immunoassays and PCR product detection,[1−3] and the ECL principles and applications have been well addressed in the literature.[4−6] In comparison with traditional laser-induced luminescence detectors, the instrumentation for ECL detection is substantially less complicated and less expensive because the excitation laser and optical filters are eliminated. Moreover, because the ECL reaction only occurs close to the surface of an electrode, the interrogated volume can be controlled and the sample requirement is quite small. This makes it an ideal detection method for microdevices, for example, for the detection of co-reactants in the ECL reaction via microchip electrophoresis.[7]

Another important area in which ECL detection has been utilized on microdevices is in DNA microarray chips, where immobilized oligonucleotide probes are used to screen DNA-containing solutions for the presence of specific target sequences. DNA from *Bacillus anthracis* has been labeled and detected in this manner using probe DNA immobilized on gold electrodes.[8] This follows the traditional method for detection in DNA arrays where the target DNA in the sample must be tagged with a fluorescent or ECL label. The labeling is normally incorporated into the amplification step to generate sufficient copies of the target DNA for detection. While the amplification/labeling step adds to the processing time, it is necessary for acquiring the needed sensitivity; however, this step could be eliminated if a modified detection method with high sensitivity were available. ECL could be such a modified detection method; it provides the necessary sensitivity and low background when utilized in a competitive hybridization assay format that would circumvent labeling of the sample DNA.

Competition assays with LIF detection utilize a fluorescent label on the probe and a quencher attached to a complementary strand that is displaced if the target sequence is present in the sample. Unlike photoluminescence quenching, however, the investigation of ECL quenching has been very limited. Richter et al.[9] reported the quenching of ECL by phenols, hydroquinones, catechol, and benzoquinones. The suggested quenching mechanism involved benzoquinone derivatives formed at the electrode surface that quenched ECL via energy transfer. When the phenol quencher was covalently bound to an oligonucleotide containing an ECL reporter, only about 50% of the ECL intensity was quenched.[10] This lacked the quenching efficiency required for quantifying DNA through hybridization. Wilson

[†] University of Virginia.
[‡] University of Virginia Health Science Center.

(1) Ohlin, M.; Silvestri, M.; Sundqvist, V.; Borrebaeck, C. A. K. *Clin. Diag. Lab. Immun.* **1997**, *4*, 107−111.
(2) DiCesare, J.; Grossman, B.; Katz, E.; Picozza, E.; Ragusa, R.; Woudenberg, T. *BioTechniques* **1993**, *15*, 152−157.
(3) Yu, H.; Bruno, J. G.; Cheng, T.; Calomiris, J. J.; Goode, M. T.; Gatto-Menking, D. L. *J. Biolumin. Chemilum.* **1995**, *10*, 239−245.
(4) Bard, A. J. *Electrogenerated Chemiluminescence*, Marcel Dekker: New York, 2004.
(5) Richter, M. M. *Electrochemilum. Chem.* **2004**, *104*, 3003−3036.
(6) Fahnrich, K. A.; Pravda, M.; Guilbault, G. G. *Talanta* **2001**, *54*, 531−559.
(7) Cao, W.; Liu, J.; Yang, X.; Wang, E. *Electrophoresis* **2002**, *23*, 3683−3691.
(8) Miao, W.; Bard, A. J. *Anal. Chem.* **2003**, *75*, 5825−5834.
(9) McCall, J.; Alexander C.; Richter, M. M. *Anal. Chem.* **1999**, *71*, 2523−2527.
(10) Richter, M. M.; Powell, M. J.; Belisle, C. M. WO 98/53316.

10.1021/ja060162g CCC: $33.50

and Johansson[11] reported highly efficient photoluminescence quenching via Förster resonance energy transfer (FRET) of $Ru(bpy)_3^{2+}$ by Black Hole Quencher-2 labeled on a DNA primer. However, this failed to quench the ECL of $Ru(bpy)_3^{2+}$ because the quencher was oxidized by the electrode before ECL began.[11] Bard and co-workers[12] reported that ECL could be quenched by 1,1′-dimethyl-4,4′-bipyridine dication (MV^{2+}) via an electron-transfer mechanism in which MV^{2+} reacted with $Ru(bpy)_3^{2+*}$ to form $Ru(bpy)_3^{3+}$ and MV^+; the MV^+ was then reoxidized to MV^{2+} at the working electrode. In addition, they reported intramolecular quenching of the ECL when the MV^{2+} was covalently bound to the ligand of $Ru(bpy)_3^{2+}$, as well as intermolecular quenching of the MV^{2+} in solution with the $Ru(bpy)_3^{2+}$. Problems with this system were later reported[13] where light was generated at the electrode in the presence of the quencher, which was due to the presence of oxygen causing reduction products of the viologen to be formed at the electrode. Obviously, achieving reproducible, high efficiency quenching requires that the quencher be not only efficient but also stable near the electrode during the ECL process at the required potential (as high as 1.2 V vs Ag/AgCl).

Metal complexes, such as $Fe(CN)_6^{3-}$, $Fe(CN)_6^{4-}$, ferrocene (Fc), and $Co(bpy)_3^{2+}$, show excellent characteristics for photoluminescence quenching of $Ru(bpy)_3^{2+}$ via either a FRET or a charge-transfer mechanism.[14−16] An energy transfer mechanism has been proposed for Fc photoluminescence quenching of $Ru(bpy)_3^{2+}$ by Alsfasser et al.,[17] who report intramolecular quenching via covalent conjugation of Fc on the $Ru(bpy)_3^{2+}$ ligand. In addition, Fc showed reversible electrochemical behavior in both organic solvent and aqueous solution, suggesting that use of this compound for ECL quenching would be possible.

In the current work, we show effective ECL quenching of $Ru(bpy)_3^{2+}$ through what is believed to be a charge transfer quenching mechanism and interference of the radical reactions. We suggest that Fc^+, the oxidative product of Fc at the electrode, reacts with excited-state $Ru(bpy)_3^{2+*}$ to quench ECL light emission. This quenching reaction was utilized in an intermolecular manner between an Fc-labeled oligonucleotide and a complementary sequence labeled with $Ru(bpy)_3^{2+}$, providing evidence that the ECL quenching method could be applied to DNA hybridization assays. Additional DNA assays that rely on photoluminescence, such as quantitative real-time PCR, could also benefit from this ECL quenching method.

Experiment Section

Materials. Tris(2,2′-bipyridyl)ruthenium(II) chloride, tripropylamine (TPA) (99%), ferrocene methanol (FcMeOH) (99%), ferrocenium hexafluorophosphate, ferrocene acetic acid (98%), phenol (99%), bis-(2,2′-bipyridine)-4′-methyl-4-carboxybipyridine ruthenium(II) chloride, *N*-succinimidyl ester bis(hexafluorophosphate), *N*,*N*′-dicyclohexylcarbodiimide (DCC), and dioxane (HPLC grade) were purchased from Sigma (St. Louis, MO) and used as received. *N*-Hydroxysuccinimide (NHS), ZONYL fluorosurfactant (FSN) (40% $F(CF_2CF_2)_{3-8}CH_2CH_2O(CH_2CH_2O)_xH$/30% 2-propanol/30% H_2O) was purchased from Aldrich (Milwaukee, WI) and heated to ∼80 °C to remove 2-propanol from the solution. Oligonucleotides modified with an amine group at the appropriate position were obtained from MWG-Biotech (High Point, NC). Other chemicals were analytical reagent grade and used as received. All solutions were prepared with water treated with a Nanopure system (Barnstead/Thermolyne, Dubuque, IA). The ECL solution, containing 0.15 M phosphate buffer and 0.1 M TPA, was adjusted with concentrated NaOH or phosphoric acid to pH 7.5 before use.

Electrochemical and ECL Measurement. Cyclic voltammetry (CV) was performed with a model 264A polarographic analyzer/stripping voltameter (EG&G Princeton Applied Research). A 2 mm diameter gold electrode was employed as a working electrode. A homemade Ag/AgCl electrode was used as a reference electrode, and a coiled gold wire served as a counter electrode. The working electrode was polished with 0.1 μm alumina slurry to obtain a mirror surface, then sonicated and thoroughly rinsed with deionized water. Before each experiment, the working electrode was subjected to repeat scanning in the potential ranges of −0.65 to 1.2 V in 0.1 M phosphate buffered saline solution until reproducible voltammograms were obtained. The solution was then replaced with the test mixture, containing the desired concentration of TPA with $Ru(bpy)_3^{2+}$ and quencher (Fc or Fc^+), or the oligonucleotides labeled with the Fc and $Ru(bpy)_3^{2+}$ species. Because of the poor solubility of ferrocene in aqueous solution, FcMeOH was used in all experiments. To realize ECL at a lower potential, 0.02% of FSN was added to the ECL solution. Along with CV measurements on the test solutions, the ECL signals were measured with a photomultiplier tube (PMT, Hamamatsu R928) installed under the electrochemical cell. The CV current and ECL intensity data were acquired with an in-house-generated program written in LabView (National Instruments, Austin, TX).

Spectroscopic and Lifetime Measurement. The luminescence emission intensity was measured using a Spex Fluorolog 2+2 spectrofluorometer (HORIBA Jobin Yvon Inc., Edison, NJ). A laser-pulsed method was employed for acquiring the luminescence lifetime. Samples were excited with a 337 nm VSL337 20 kW peak power, 3 ns duration, 20 pps nitrogen laser (Laser Science, Inc. Franklin, MA). The luminescence signal was detected with a photomultiplier tube, and the output was viewed on a 500 MHz TDS 540 digital oscilloscope (Tektronix, Inc., Beaverton, Oregon) and transferred to an interfaced computer. Absorption data were determined with a Hewlett-Packard 8452A diode array spectrometer.

DNA Labeling. Complementary oligonucleotides, 23 base pairs in length, were modified to determine the efficiency of intramolecular quenching in a DNA hybridization assay. The oligonucleotide with sequence 5′-GAT GAG TTC CTG TCC GTA CAA CT-3′ was labeled with $Ru(bpy)_3^{2+}$ at the 5′-end through an amino modification containing a six carbon spacer arm. The labeling and purification of the $Ru(bpy)_3^{2+}$−oligonucleotide was performed according to a previously published method.[18] The purified product was confirmed by MALDI-TOF MS. The complementary oligonucleotide with sequence 5′-AGT TGT ACG GAC ACG AAC TCA TC-3′ was labeled at the 3′-end through an amino modification containing a three carbon spacer arm. Synthesis of the *N*-hydroxysuccinimide ester of ferrocene acetic acid and subsequent synthesis of the ferrocenyl oligonucleotide were completed as described by Takenaka et al.[19] The purified ferrocenyl oligonucleotide was confirmed by MALDI-TOF MS. Hybridization experiments were performed by mixing complementary DNA solutions and incubating at room temperature for 30 min before detection.

(11) Wilson, R.; Johansson, M. K. *Chem. Commun.* **2003**, *21*, 2710−2711.
(12) Xu, X.; Shreder, K.; Iverson, B. L.; Bard, A. J. *J. Am. Chem. Soc.* **1996**, *118*, 3656−3660.
(13) Clark, C. D.; Debad, J. D.; Yonemoto, E. H.; Mallouk, T. E.; Bard, A. J. *J. Am. Chem. Soc.* **1997**, *119*, 10525−10531.
(14) Liu, D. K.; Brunschwig, B. S.; Creutz, C.; Sutin, N. *J. Am. Chem. Soc.* **1986**, *108*, 1749−1755.
(15) Demas, J. N.; Addington, J. W. *J. Am. Chem. Soc.* **1976**, *98*, 5800−5806.
(16) Navon, G.; Sutin, N. *Inorg. Chem.* **1974**, *13*, 2159−2164.
(17) Geisser, B.; Alsfasser, R. *Inorg. Chim. Acta* **2003**, *344*, 102−108.
(18) Gudibande, S. R.; Kenten, J. H.; Link, J.; Friedman, K.; Massey, R. J. *Mol. Cell. Probes* **1992**, *6*, 495−503.
(19) Takenaka, S.; Uto, Y.; Kondo, H.; Ihara, T.; Takagi, M. *Anal. Biochem.* **1994**, *218*, 436−443.

Results and Discussion

Since the ECL of $Ru(bpy)_3^{2+}$ is generated at a relatively high potential, an ECL quencher must be stable on the electrode during the ECL reaction in order to achieve high efficiency and reproducible quenching results. However, most of the organic quenchers of $Ru(bpy)_3^{2+}$ luminescence, such as black hole quenchers, cannot exist stably on the electrode during the ECL reaction. Ferrocene is a well-known quencher of $Ru(bpy)_3^{2+}$ luminescence; it is oxidized at 0.31 V vs SCE to form ferrocenium, which also quenches $Ru(bpy)_3^{2+}$ luminescence through electron transfer. Since ferrocenium/ferrocene are quite stable species at the electrode during the ECL time scale, we explored the ability of ferrocene to quench $Ru(bpy)_3^{2+}$ ECL.

$Ru(bpy)_3^{2+}$ ECL Quenched by FcMeOH. A typical ECL intensity−potential plot for the $Ru(bpy)_3^{2+}$−TPA system (with a $Ru(bpy)_3^{2+}$ concentration of 10.0 μM) is presented in Figure 1A. Two ECL peaks were observed while sweeping the potential from 0 to 1.4 V. The first peak began to appear at 0.85 V and reached a maximum at 1.0 V. The intensity of this low potential (1.0 V) peak was much weaker than that of the second peak at a higher potential of 1.2 V. The reported mechanism of generating excited-state $Ru(bpy)_3^{2+}$ in the presence of the TPA co-reactant at the lower potential is shown in Scheme 1.The model attributes the lower potential ECL to direct oxidation of TPA to TPA$^{\cdot+}$, which deprotonates to form TPA$^{\cdot}$. The TPA$^{\cdot}$ radical species reduces $Ru(bpy)_3^{2+}$ to form $Ru(bpy)_3^{+}$, which further reacts with the oxidative species, TPA$^{\cdot+}$, to form $Ru(bpy)_3^{2+*}$.[20,21]

Onset of the second luminescence peak occurred at 1.05 V and reached a maximum at 1.2 V. ECL at the higher potential is attributed to direct oxidization of $Ru(bpy)_3^{2+}$ on the electrode to form $Ru(bpy)_3^{3+}$, which further reacts with the TPA$^{\cdot}$ radical species to generate $Ru(bpy)_3^{2+*}$,[22,23] as shown in Scheme 2. An alternative mechanism for generating $Ru(bpy)_3^{2+*}$ at the higher potential is through the direct TPA oxidation given in Scheme 1. It is also possible that $Ru(bpy)_3^{3+}$ generated in Scheme 2 reacts with $Ru(bpy)_3^{+}$ generated in Scheme 1 to form $Ru(bpy)_3^{2+*}$. The importance of the contribution of each of these mechanisms for formation of the excited state is not known.

To investigate quenching of the $Ru(bpy)_3^{2+}$ ECL by ferrocene, the more soluble ferrocene methanol (FcMeOH) species was utilized, but the redox potential difference between Fc/Fc^{+} [24] and $FcMeOH/FcMeOH^{+}$ [25] is small enough to be neglected. As seen in Figure 1A, the presence of 100 μM of FcMeOH in a 10 μM $Ru(bpy)_3^{2+}$ solution shifted the high potential ECL peak to 1.3 V with 78% of ECL being quenched. The intensity of the ECL at 1.0 V decreased to 12% of that in the absence of FcMeOH. Since the solution layer through which the emitted light passes is very thin (less than 0.5 mm), the decrease in ECL attributed to FcMeOH absorbance can be ignored. Meanwhile, compared with the anionic current for ECL in the absence of Fc, anionic current corresponding to the ECL reaction in the presence of quencher showed no obvious change.

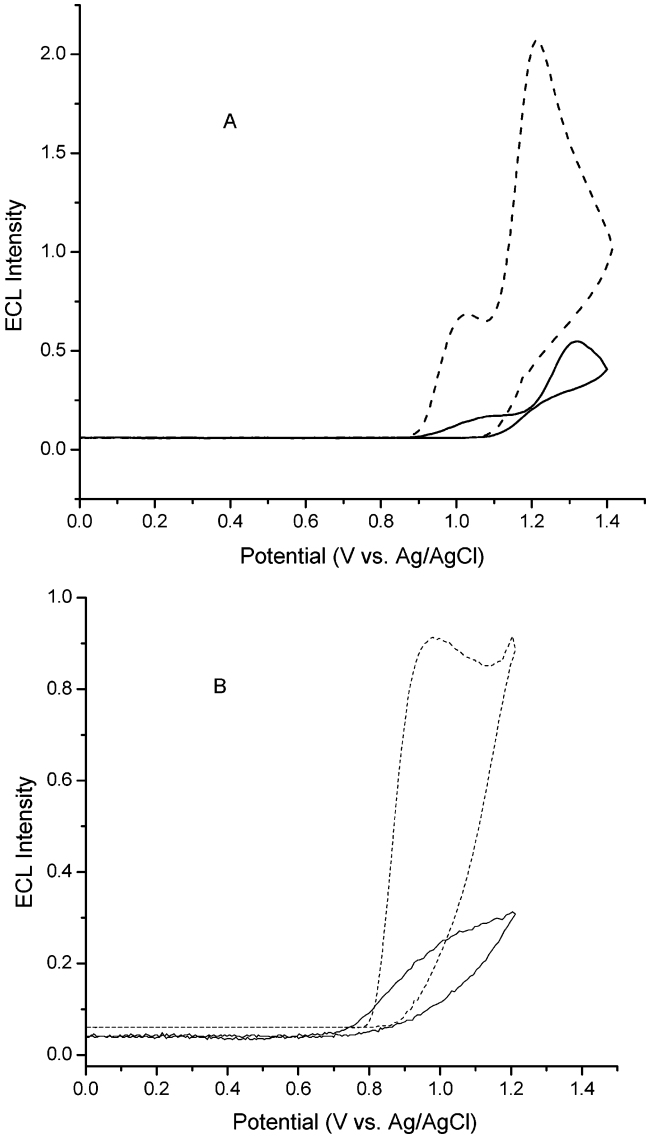

Figure 1. (A) ECL emission−potential transients at the gold electrode in 0.15 M phosphate buffer (pH 7.4) containing 0.1 M TPA in the absence (dotted line) and presence of 100 μM FcMeOH (solid line). (B) ECL emission−potential transients at a gold electrode in 0.15 M phosphate buffer (pH 7.4) containing 0.1 M TPA and 0.02% FSN in the absence (dotted line) and presence (solid line) of 100 μM FcMeOH. The $Ru(bpy)_3^{2+}$ concentration is 10 μM, and the scan rate is 100 mV/s.

Scheme 1

$$TPA - e \rightarrow TPA^{\cdot+} \quad (1)$$

$$TPA^{\cdot+} \rightarrow TPA^{\cdot} + H^{+} \quad (2)$$

$$TPA^{\cdot} + Ru(bpy)_3^{2+} \rightarrow Ru(bpy)_3^{+} + \text{product} \quad (3)$$

$$Ru(bpy)_3^{+} + TPA^{\cdot+} \rightarrow Ru(bpy)_3^{2+*} + \text{product} \quad (4)$$

Scheme 2

$$Ru(bpy)_3^{2+} - e \rightarrow Ru(bpy)_3^{3+} \quad (5)$$

$$TPA - e \rightarrow TPA^{\cdot+} \quad (6)$$

$$TPA^{\cdot+} \rightarrow TPA^{\cdot} + H^{+} \quad (7)$$

$$Ru(bpy)_3^{3+} + TPA^{\cdot} \rightarrow Ru(bpy)_3^{2+*} \quad (8)$$

Li and Zu[26] reported that, in the presence of the nonionic fluorosurfactant FSN, ECL intensity at the lower potential (0.9−1.0 V) was dramatically increased, achieving levels higher than

(20) Miao, W.; Choi, J.-P.; Bard, A. J. *J. Am. Chem. Soc.* **2002**, *124*, 14478−14485.
(21) Zu, Y.; Bard, A. J. *Anal. Chem.* **2000**, *72*, 3223−3232.
(22) Rubinstein, I.; Bard, A. J. *J. Am. Chem. Soc.* **1981**, *103*, 512−516.
(23) Leland, J. K.; Powell, M. J. *J. Electrochem. Soc.* **1990**, *137*, 3127−3131.
(24) Bard, A. J.; Faulkner, L. R. *Electrochemical Methods: Fundamentals and Applications*, 2nd ed.; Wiley: New York, 2000; p 811.
(25) Creager, S. E.; Rowe, G. K. *Anal. Chim. Acta* **1991**, *246*, 233−239.
(26) Li, F.; Zu, Y. *Anal. Chem.* **2004**, *76*, 1768−1772.

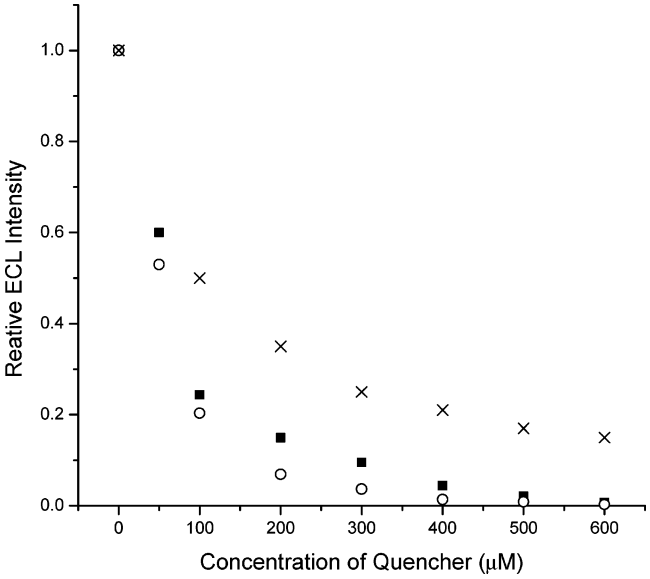

Figure 2. ECL intensity versus quencher concentration for phenol at 1.2 V (×), FcMeOH at 1.2 V (■), and FcMeOH at 0.95 V in the presence of 0.02% FSN (○), on the gold electrode in 0.15 M phosphate buffer (pH 7.4) containing 0.1 M TPA. The $Ru(bpy)_3^{2+}$ concentration is 10 μM, and the scan rate is 100 mV/s.

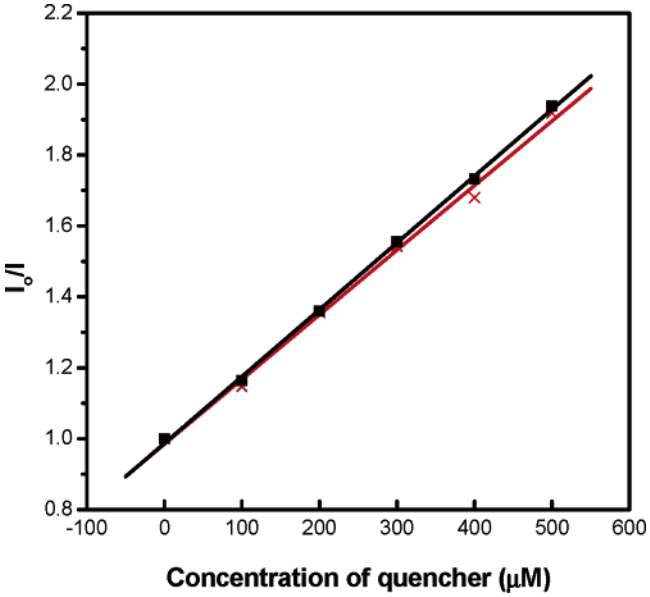

Figure 3. Intensity Stern−Volmer photoluminescence quenching plot for 10 μM $Ru(bpy)_3^{2+}$ by FcMeOH (×) and $FcMeOH^+$ (■) in 0.1 M H_2SO_4 in the absence of oxygen.

that observed at 1.2 V. This is attributed to adsorption of the hydrophobic fluorinated chains adjacent to the surface of the gold electrode, providing a favorable environment for producing $Ru(bpy)_3^{+}$. As seen in Figure 1B, the presence of 0.02% FSN in the solution dramatically increased the intensity of the ECL while scanning the potential from 0.7 to 1.0 V. In the presence of the surfactant, ECL emission started at 0.78 V and reached a maximum at 0.95 V. The quenching effect of 100 μM FcMeOH at the lower potential in the presence of the surfactant is also presented in Figure 1B. With FcMeOH added, the ECL intensity increased with potential, but there was no obvious peak observed at ~0.95 V. The ECL intensity at 0.95 V decreased to 20% of that in the absence of FcMeOH. In addition, little anodic current change corresponding to the ECL was observed during quenching. The ratio of the cathodic current to the anodic current of Fc was measured to be 0.98, suggesting that FcMeOH/$FcMeOH^+$ is stable during ECL.

The same quenching efficiency observed in 10 μM $Ru(bpy)_3^{2+}$ was also seen in 1.0 and 0.2 μM $Ru(bpy)_3^{2+}$ concentrations in the presence of 100 μM of FcMeOH at both the low potential and high potential. This indicated that over a wide range the quenching efficiency did not depend on the ratio of $Ru(bpy)_3^{2+}$ to FcMeOH. To determine the effect of the quencher concentration, titration of 10 μM $Ru(bpy)_3^{2+}$ with FcMeOH was investigated at 1.2 V in the absence of FSN and at 0.95 V in the presence of FSN. These results are shown in Figure 2 along with results from experiments employing phenol as the quenching agent. FcMeOH quenching of ECL occurring at the two different potentials has similar effects with the ECL intensity dramatically decreasing with increasing FcMeOH concentration. When 500 μM FcMeOH was present in the ECL solution, the ECL intensity was decreased by greater than 99%. For comparison, the phenol quenching of ECL showed a signal decrease of 40% when 100 μM of phenol was included in the ECL solution, versus the 78−80% decrease observed with the same concentration of FcMeOH; this efficiency for FcMeOH quenching of ECL was similar at both the low and high potential. The quenching efficiency of FcMeOH is also higher than that of MV^{2+} as reported by Bard et al.,[12] where 500 μM MV^{2+} quenched about 50% of the light emission from 6.0 μM $Ru(bpy)_3^{2+}$.

$Ru(bpy)_3^{2+}$ Luminescence Quenching by $FcMeOH^+$/FcMeOH Species. To allow determination of the ECL quenching mechanism, experiments were performed on the luminescent quenching of $Ru(bpy)_3^{2+}$ by FcMeOH and $FcMeOH^+$ using both steady-state and time-resolved luminescence methods. Since Fc^+ is not stable in neutral aqueous solution over the extended measurement period, these quenching experiments were completed in 0.1 M sulfuric acid solution. Each solution was deoxygenated with nitrogen gas for 20 min before a measurement. The results of the concentration study experiments are presented as Stern−Volmer plots for FcMeOH and Fc^+ in Figure 3. The data were corrected by means of the equation:[27,28]

$$\left(\frac{I_0}{I}\right)_{\text{corr}} = \left(\frac{I_0}{I}\right)_{\text{app}}\left[\frac{1-10^{-(A_D+A_Q)l}}{1-10^{-A_D l}}\right]\frac{A_D 10^{-A_Q' l'}}{A_D + A_Q} \qquad (9)$$

where $(I_0/I)_{\text{app}}$ is the observed ratio of luminescence intensity in an unquenched sample to that in a quenched one, and $(I_0/I)_{\text{corr}}$ is the ratio corrected for the trivial absorption of the excitation and emitted light by the solution. A_D and A_Q are the absorbances per centimeter at the excitation wavelength for the donor and the quencher, respectively; A_Q' is the absorbance of the quencher at the emission wavelength; l is the effective path length within the cell (1 cm) for absorbance of the excitation radiation, and l' is the effective path length for absorption of the emitted radiation, estimated to be 0.5 cm. FcMeOH shows an absorbance peak at 440 nm with overlap of the 467 nm excitation wavelength used for $Ru(bpy)_3^{2+}$; ϵ for FcMeOH at 467 nm is 75 M^{-1} cm^{-1}. FcMeOH has no absorbance at the emission wavelength of $Ru(bpy)_3^{2+}$. For Fc^+, the absorbance

(27) Navon, G.; Sutin, N. *Inorg. Chem.* **1974**, *13*, 2159−2164.
(28) Demas, J. N.; Admson, A. W. *J. Am. Chem. Soc.* **1973**, *95*, 5159−5168.

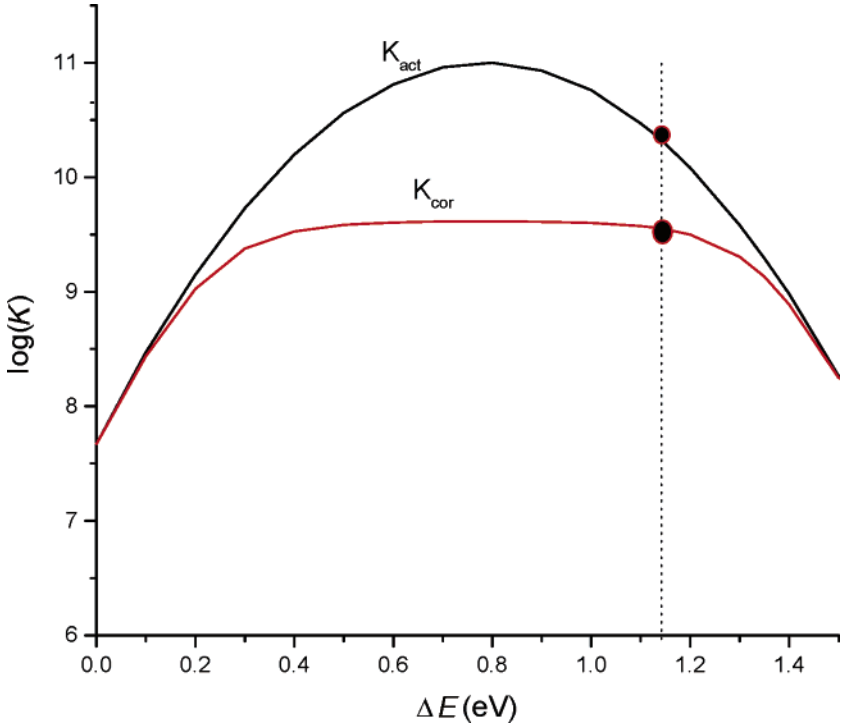

Figure 4. Parabolic dependence of the electron-transfer rate on potential. Points indicate the actual driving force in the $Ru(bpy)_3^{2+*}/FcMeOH^+$ system under both free and diffusion-controlled conditions.

band spans 550−650 nm, which significantly overlaps the emission spectrum of $Ru(bpy)_3^{2+}$; $\epsilon(Fc^+)_{610}$ is 356 M^{-1} cm^{-1}.

As illustrated in Figure 3, FcMeOH and $FcMeOH^+$ give similar luminescence quenching of $Ru(bpy)_3^{2+}$. In the presence of 100 μM of FcMeOH or $FcMeOH^+$, 12% of $Ru(bpy)_3^{2+}$ luminescence was quenched. Using the intensity values from the Stern−Volmer plots for FcMeOH and $FcMeOH^+$ given in Figure 3, and the photoluminescence lifetime of $Ru(bpy)_3^{2+}$ in the absence of quencher of 589 ns, a value for K_{SV} of 1820 M^{-1}, corresponding to a k_q of 3.1×10^9 M^{-1} s^{-1}, was determined for FcMeOH. This value is in excellent agreement with the value of 3.1×10^9 M^{-1} s^{-1} reported for quenching in DMF solution.[29] The intensity Stern−Volmer plot for $FcMeOH^+$ gives a K_{SV} of 1880 M^{-1}, corresponding to a k_q of 3.6×10^9 M^{-1} s^{-1}. The fluorescent quenching rate constants for both FcMeOH and $FcMeOH^+$ are close to the diffusion control limit. Compared with luminescence quenching by FcMeOH or $FcMeOH^+$, the ECL quenching efficiency by FcMeOH was much higher. For 100 μM of FcMeOH quencher, the ECL intensity was quenched by 80%, while the luminescence intensity was only quenched by 12%.

Both energy transfer and electron-transfer quenching of the $Ru(bpy)_3^{2+}$ luminescence can occur.[30] The dominant mode depends on the redox properties of the ferrocene.[31−34] Because of the large driving force, we favor excited-state electronic transfer quenching by $FcMeOH^+$, but the detailed mechanism is unimportant so long as it is fast and efficient.

Mechanism of Fc Quenching of ECL. According to the Marcus bimolecular electron transfer theory, the activated electron-transfer rate constant between $FcMeOH^+$ and $Ru(bpy)_3^{2+*}$ can be simply described by eqs 10−12.[35]

$$k_{act} = (k_{11}K_{12}k_{22}f)^{1/2} \tag{10}$$

$$\ln f = \frac{(\ln K_{12})^2}{4\ln(k_{11}k_{22}/Z^2)} \tag{11}$$

$$K_{12} = e^{nF/RT\Delta E^0} \tag{12}$$

where k_{11} and k_{22}, the exchange rate constants for Fc^+−Fc and $Ru(bpy)_3^{2+*}$−$Ru(bpy)_3^{3+}$, are 5.3×10^6 [36] and 4.2×10^8 M^{-1} s^{-1},[37] respectively. Z, the frequency of collision between two molecules with a solvent cage, is taken as 10^{11} M^{-1} s^{-1}. Using these values, k_{act} versus ΔE^0 has been calculated and is presented in Figure 4. The reorganization energy from this graph is 0.8 eV. For $Ru(bpy)_3^{3+}/Ru(bpy)_3^{2+*}$ and Fc^+/Fc, the values of E^0 are −0.83 and 0.31 V vs SCE, respectively, giving a ΔE^0 of 1.14 V; the k_{act} at this potential is indicated in Figure 4. On the basis of the graph in Figure 4, it is seen that the electron transfer between $FcMeOH^+$ and $Ru(bpy)_3^{2+*}$ is located in the Marcus Inverted Region. The k_{act} between $FcMeOH^+$ and $Ru(bpy)_3^{2+*}$ is calculated to be 2.1×10^{10} M^{-1} s^{-1}. As expected, the photoluminescence quenching rate constant is much lower than k_{act} since it is under the effect of diffusion control. The diffusion-controlled rate constant (7.4×10^9 M^{-1} s^{-1}) was corrected by

(29) Ollino, M.; Cherry, W. R. *Inorg. Chem.* **1985**, *24*, 1417−1418.
(30) Lee, E. L.; Wrighton, M. S. *J. Am. Chem. Soc.* **1991**, *113*, 8562−8564.
(31) Xia, X.; Ding Z.; Liu, J. *J. Photochem. Photobiol. A: Chem.* **1995**, *88*, 81−84.
(32) Duan, C.; Zhu, L.; You, X. *Chin. Sci. Bull.* **1993**, *38*, 462−466.
(33) Kitamura, N.; Kawanishi, Y.; Tazuke, S. *Chem. Phys. Lett.* **1983**, *97*, 103−106.
(34) Bard, A. J.; Faulkner, L. R. *Electrochemical Methods: Fundamentals and Applications*, 2nd ed.; Wiley: New York, 2000; p 763.
(35) Marcus, R. A. *J. Chem. Phys.* **1965**, *43*, 679−701.
(36) Kevin, R.; Howes, C.; Greg, P.; James, C.; Sullivan, D. M.; James, H. E.; Andreja, B. *Inorg. Chem.* **1988**, *27*, 2932−2934.
(37) Navon, G.; Sutin, N. *J. Am. Chem. Soc.* **1979**, *101*, 883−892.

the Debye equation:[38]

$$k_{diff} = 10^c(7.4 \times 10^9)b(e^b - 1) \quad (13)$$

$$b = 14Z_1Z_2/a \quad (14)$$

$$c = Z_1Z_2\mu^{1/2}/(1 + \mu^{1/2}) \quad (15)$$

wherein Z_1 and Z_2 are the charges of $FcMeOH^+$ and $Ru(bpy)_3^{2+}$, and a is the distance of closest approach in angstroms (Å). The radii of $FcMeOH^+$ and $Ru(bpy)_3^{2+}$ are 3.5[39] and 6.8 Å.[34] Therefore, a is estimated to be 10.3 Å in aqueous solution. With the ionic strength of the solution, μ, taken as 0.1 M, k_{diff} is calculated to be $4.3 \times 10^9\ M^{-1}\ s^{-1}$. The correction for diffusion control was performed using the equation[40]

$$k_{corr} = k_{act}k_{diff}/(k_{act} + k_{diff}) \quad (16)$$

The plot of k_{corr} versus the free energy driving force is also shown in Figure 4. Limited by diffusion control, the corrected electron-transfer rate constant between $FcMeOH^+$ and $Ru(bpy)_3^{2+}$, k_{corr}, is $3.6 \times 10^9\ M^{-1}\ s^{-1}$, which is in good agreement with the measured rate constants obtained from the photoluminescence quenching experiment.

Light emission of $Ru(bpy)_3^{2+}$ ECL is generated by a chemical reaction triggered by the electrochemical reaction, and ferrocene is oxidized to ferrocenium at the electrode; thus, the ECL quenching mechanism is more complicated than photoluminescence quenching. At the potential required to generate ECL of $Ru(bpy)_3^{2+}$, Fc is oxidized to form stable Fc^+ at the electrode, thus under ECL condition, the dominant form of ferrocene at the electrode is $FcMeOH^+$. In accordance with the results of Xia et al.[31] for photoluminescence quenching, we propose the ECL quenching mechanism shown in Scheme 3, in which the stable $FcMeOH^+$ quenches ECL of $Ru(bpy)_3^{2+}$ through an electron-transfer mechanism.

Scheme 3

$$FcMeOH - e \rightarrow FcMeOH^+ \quad \text{electrode} \quad (17)$$

$$FcMeOH^+ + Ru(bpy)_3^{2+*} \rightarrow FcMeOH + Ru(bpy)_3^{3+} \quad (18)$$

While this certainly contributes to the ECL quenching, it cannot be the entire picture. The degree of ECL quenching is much higher than that predicted by the diffusion-controlled rate constant.

The enhanced quenching of the ECL can be explained by radical reactions. In ECL, $FcMeOH^+$ can inhibit generation of $Ru(bpy)_3^{2+*}$. In the low potential ECL, $Ru(bpy)_3^{2+*}$ is generated from $TPA^{\bullet+}$ reacting with $Ru(bpy)_3^+$ (eq 4). Electrogenerated $FcMeOH^+$ can compete with the $TPA^{\bullet+}$ oxidation of $Ru(bpy)_3^+$, but the ΔE between Fc^+ ($E^0_{Fc^+/Fc} = 0.31$V vs SCE) and $Ru(bpy)_3^+$ (−1.4V vs SCE)[41] is too small to generate $Ru(bpy)_3^{2+*}$. This reaction does quench the luminescence by lowering the concentration of $Ru(bpy)_3^+$ available to form $Ru(bpy)_3^{2+*}$.

In the high potential region, where the ECL mechanism is different, another radical reaction can account for the enhanced ECL quenching. The oxidizing $FcMeOH^+$ can compete with $Ru(bpy)_3^{3+}$ and $Ru(bpy)_3^{2+}$ in reacting with the highly reducing $TPA^{\bullet}$. This mechanism is well established in other ECL systems and can account for Stern−Volmer quenching constants that are much larger for ECL than for photoluminescence.[42] We attribute the remainder of the ECL quenching to this mechanism.

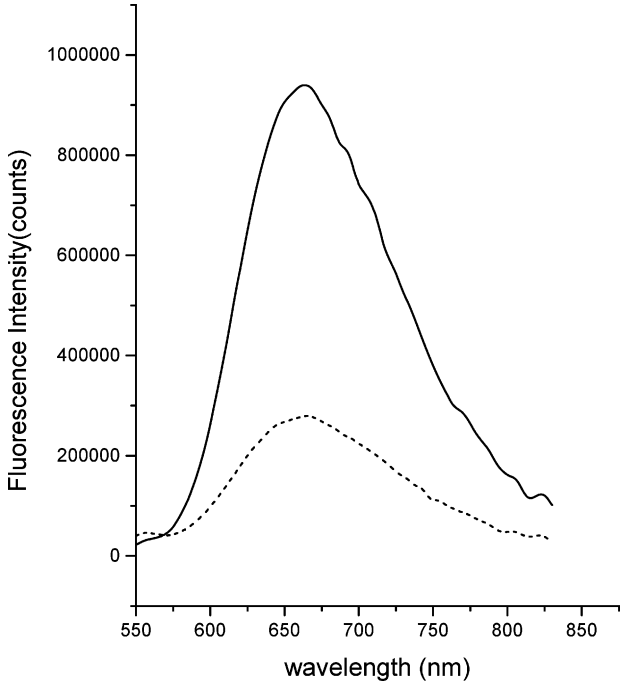

Figure 5. Photoluminescence assay of 1.0 μM $Ru(bpy)_3^{2+}$-labeled oligonucleotide before (solid line) and after addition of 1.0 μM of complementary DNA labeled with Fc. The excitation wavelength is 467 nm.

Intramolecular Quenching in Oligonucleotide Probes. With a view to the possibility of utilizing the quenching ability of ferrocene in DNA hybridization detection, quenching experiments were performed utilizing a set of 23 base pair complementary oligonucleotides. The luminescence emission of a 1.0 μM solution of $Ru(bpy)_3^{2+}$ covalently attached to a DNA strand is shown in Figure 5 with 467 nm excitation. The maximum photoluminescence intensity of the $Ru(bpy)_3^{2+}$ labeled on the DNA was 650 nm, significantly shifted from the 610 nm maximum observed with free $Ru(bpy)_3^{2+}$. The lifetime of photoluminescence was 370 ns. When 1.0 μM of a complementary DNA strand, labeled with Fc, was added to the solution and incubated for 30 min, the luminescence intensity decreased by 78% (Figure 5), while the photoluminescence lifetime remained unchanged at 370 ns. Addition of 10 μM FcMeOH to the 1.0 μM DNA−$Ru(bpy)_3^{2+}$ solution did not cause obvious quenching, indicating that intramolecular quenching by the Fc conjugated on the 3′-end of the complementary DNA strand was occurring.

A similar quenching behavior was observed in ECL experiments with the labeled oligonucleotides, as shown in Figure 6. The ECL intensity of $Ru(bpy)_3^{2+}$-labeled DNA was observed as the potential was scanned from 0 to 1.3 V vs Ag/AgCl in the absence of FSN. When an equivalent concentration of the complementary Fc-labeled DNA sequence was added and incubated for 30 min, the ECL intensity at 1.2 V was quenched by 95%. As shown in Figure 7, the quenched intensity was linear with the amount of Fc-labeled DNA sequence added to the solution. Fitting these data established that ECL quenching of

(38) Debye, P. *Trans. Electrochem. Soc.* **1942**, *82*, 268.
(39) Pladziewicz, J. R.; Espenson, J. H. *J. Am. Chem. Soc.* **1973**, *95*, 56−63.
(40) Lin, C.-T.; Böttcher, W.; Chou, M.; Creutz, C.; Sutin, N. *J. Am. Chem. Soc.* **1976**, *98*, 6536−6544.
(41) White, H. S.; Bard, A. J. *J. Am. Chem. Soc.* **1982**, *104*, 6891−6895.

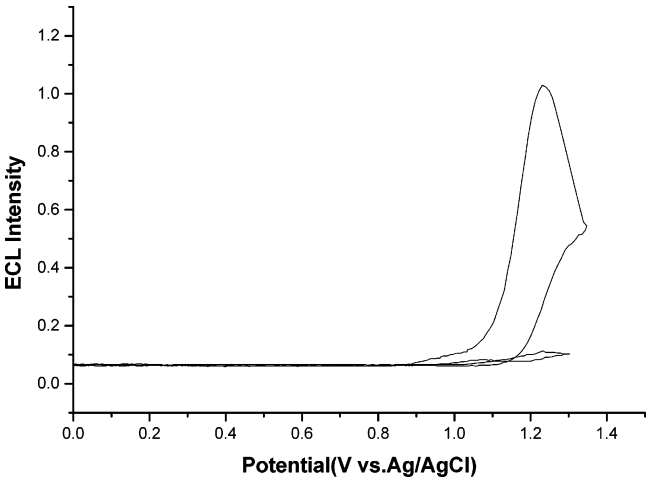

Figure 6. ECL assay of 1.0 μM $Ru(bpy)_3^{2+}$-labeled oligonucleotide before (solid line) and after addition of 1.0 μM of complementary DNA labeled with Fc.

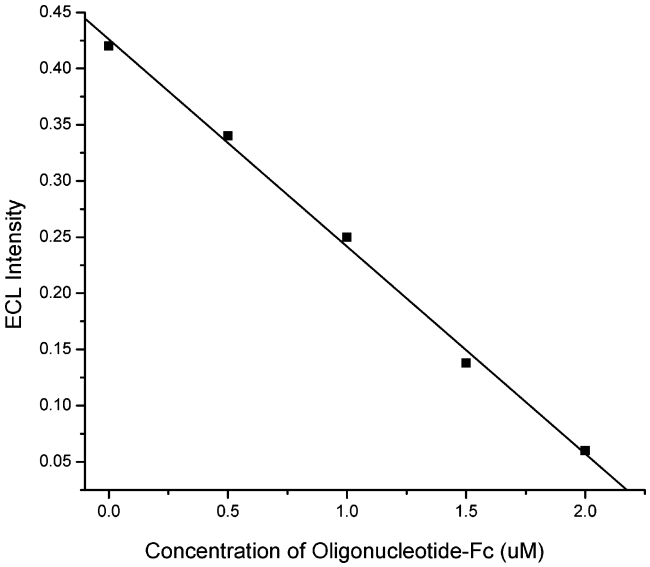

Figure 7. Dependence of 2.0 μM $Ru(bpy)_3^{2+}$-labeled oligonucleotide ECL intensity on the concentration of Fc-labeled DNA.

the Fc-labeled duplex was complete and that the association constant for the complementary duplexes was $>50\ \mu M^{-1}$.

The electron transfer is believed to occur between the $Ru(bpy)_3^{2+*}$ and the $FcMeOH^+$ species because the complementary DNA sequences bring the ECL reporter and the quencher molecule into close proximity. It is known that, in 5′-end-labeled doubled-stranded DNA, the chromophore is associated with the DNA by end capping, that is, the chromophore is stacked at the end of the helix in a manner similar to that of an additional base pair.[43] ECL quenching is then expected to occur through direct electron transfer from the $Ru(bpy)_3^{2+}$ to the quencher molecule. An alternative possibility is that quenching takes place via charge transfer through the base pairs of the DNA to the quencher molecule. Testing of this possibility will require labeling of both oligonucleotide strands at the 5′-end to prevent direct interaction of the reporter and quencher, while still allowing charge transfer through the DNA.

Conclusions

Compared to other well-established ECL quenchers, ferrocene shows a significantly higher efficiency in quenching the ECL of $Ru(bpy)_3^{2+}$. Little current change in the CV was observed in ECL quenching with ferrocene, and the large potential difference between Fc^+ and $Ru(bpy)_3^{2+*}$ suggests that electron-transfer quenching between Fc^+ and $Ru(bpy)_3^{2+*}$ is possible. Moreover, the derived quenching rate constant is in good agreement with that predicted by Marcus theory. Differences in the quenching efficiency between ECL and photoluminescence were observed and could be explained in the ECL by both diffusional quenching and interference with the radical reactions responsible for the ECL. Using this ECL quenching mechanism, a novel intramolecular ECL quenching mechanism in complementary oligonucleotides has been observed. The quenching efficiency is virtually complete, promising the potential application of this method for application to sequence-specific DNA detection.

JA060162G

(42) Zhang, H.; Zu, Y. *J. Phys. Chem.* **2005**, 16047−16051.
(43) Kelley, S. O.; Holmlin, R. E.; Stemp, E. D. A.; Barton, J. K. *J. Am. Chem. Soc.* **1997**, *119*, 9861−9870.